A General Approach to Sampled-Data Modeling for Power Electronic Circuits

GEORGE C. VERGHESE, MEMBER, IEEE, MALIK E. ELBULUK, STUDENT MEMBER, IEEE, AND JOHN G. KASSAKIAN, SENIOR MEMBER, IEEE

Abstract—**A general sampled-data representation of the dynamics of arbitrary power electronic circuits is proposed to unify existing approaches. It leads, via compact and powerful notation, to disciplined modeling and straightforward derivation of small-signal models that describe perturbations about a nominal cyclic steady state. Its usefulness is further illustrated by considering the representation and analysis of a class of symmetries in circuit operation. The results of the application of this methodology to modeling the small-signal dynamics of a series resonant converter are described. The results correlate well with simulation results obtained on the Massachusetts Institute of Technology's Parity Simulator. What is of greater significance is the fact that the small-signal model is obtained in a completely routine way, starting from a general formulation and working down to the actual circuit; this contrasts with the circuit-specific analyses that are more typical of the power electronics literature. The automatability of this procedure is also discussed, and it is pointed out that the key ingredients for automatic generation of dynamic models from a circuit specification are now available.**

I. Introduction

A. Background

MODELS FOR THE dynamics of power electronic circuits are of crucial importance in many applications, both for assessing stability and for designing compensators to enhance stability and performance. However, the derivation of such models in the power electronics literature has typically been circuit specific, notably in the case of small-signal models. With a few significant exceptions (some of which are cited in Section II) little effort has gone into extracting and clearly exhibiting those aspects of a circuit's representation and analysis that can be carried over to other related circuits. This has led to a rather unsatisfactory state of affairs in which designers find little guidance in the literature for the task of developing small-signal models of their circuits.

B. Contributions of this Paper

A general sampled-data representation of power electronic circuit dynamics is proposed to unify existing approaches. It leads, via compact and powerful notation, to disciplined modeling and straightforward derivation of small-signal models that describe perturbations about a nominal cyclic steady state. The procedure is "top-down" and automatable. It starts from a general formulation that serves to focus the task of representing the circuit and systematically works down to the details of the circuit; this contrasts with the circuit-specific analyses mentioned earlier. Our treatment makes evident the feasibility of automating the *derivation* (and not just the analysis) of small-signal sampled-data models. The formulation also facilitates the representation and analysis of such features as symmetry in circuit operation.

A framework such as ours undoubtedly underlies, even if only implicitly, the circuit-specific analyses that have been presented in the power electronics literature. However, few attempts have been made at a clear and explicit framework of the generality aimed at in this paper. Two recent papers whose objectives and contributions overlap significantly with ours are [31] and [32]. The former predates our work, but we were unaware of it at the time the first version of the present paper was written; in [32] the first version of our present paper is referenced and extended in some ways but [32] seems not to recognize the significant overlap between itself and our work here. The viewpoints of [31], [32], and the present paper are complementary in many respects, and the reader is encouraged to examine those references as well.

C. Outline of Contents

We begin in Section II with a brief review of some previous work on the modeling and analysis of dynamics in switched dc–dc converters. This gives us a point of departure as well as a benchmark for comparison with the subsequent results. In particular, an attempt is made to identify (for emulation in a more general setting) those features that make "state-space averaging" the preferred approach to analyzing this class of circuits. Some previous work on analyzing other classes of power electronic circuits is also mentioned.

Section III introduces the representation of power electronic circuits as cyclically switched systems and develops the associated notation. Section IV then treats the nominal cyclic steady state and derives the small-signal sampled-data model for perturbations about this nominal steady state. The simplicity of the development in these

Manuscript received August 10, 1984; revised November 7, 1985. This paper was presented at the IEEE Power Electronics Specialists' Conference, Gaithersburg, MD, June 18–21, 1984. This work was supported in part by the Electrical Energy Systems Division of the U.S. Department of Energy under Contract EX-76-A-01-2295 T.O. 47H, by the MIT/Industry Power Electronics Collegium, and by a grant from the General Electric Company.

The authors are with the Laboratory for Electromagnetic and Electronic Systems, Room 10-069, Massachusetts Institute of Technology, Cambridge, MA 02139.

IEEE Log Number 8407067.

two sections illustrates the power (well-known to mathematicians and sorcerers!) that comes from an appropriate choice and use of symbols. Issues related to exploiting circuit symmetry and automating the derivation of the model are discussed in both of these sections.

The procedure of Sections III and IV is illustrated in Section V by application to a simple series resonant converter. This application originally stimulated the efforts leading to the present paper, but the application is presented here only to the extent required to illustrate the modeling procedure. The small-signal sampled-data model, obtained in a completely routine way using our framework, behaves consistently with simulation results obtained on the Massachusetts Institute of Technology's Parity Simulator, as demonstrated in that section.

II. Some Previous Work

We outline in this section some previous work on both continuous-time and sampled-data modeling of *switched dc–dc converters*, as the approaches to analysis for this category of circuits are more developed in the literature than for other categories. This will orient us suitably for the development in the remaining sections. Some reference will also be made at the end of this section to work on models for other classes of circuits.

A. Approximate Continuous-Time Models of Switched DC–DC Converters

Switched dc–dc converters are uniquely amenable to certain natural approximations, typically involving replacement of instantaneous variables by averaged quantities. This has led to many different, but essentially equivalent, approaches to developing approximate continuous-time large- and small-signal models for these circuits; see, for example, [1]–[4] and the references therein.

The clearest of these approximation approaches, and the one that seems to have become most popular, is the state-space averaging approach described in [2] and [39]. A great deal has been written on this (see, for example, the discussion and references in [5]), so it will not be reviewed here. We concentrate instead on discussing what we consider to be its strengths. (It is interesting to note, incidentally, that the basic idea of state-space averaging has been known for some time in contexts other than power electronics: "sliding modes" in switched-structure systems [6], [7] are governed by a model that results from averaging two possibly nonlinear state-space descriptions, using a duty cycle that is implicitly determined by the two descriptions and the switching law; and in so-called "relaxed-state" high-frequency periodic control of a possibly nonlinear process [8] the evolution of the relaxed state is again governed by a model obtained by averaging the description of the original process.)

State-space averaging of switched converters has the virtue of starting from a standardized and general system representation, namely a state-space description of the circuit in each of its switch configurations. This enforces a valuable discipline on the modeling process because one has a target form in mind when describing the circuit, and one has the assurance that the circuit description can be brought to this target form. Second, and as a consequence of the first feature, the development of an approximate small-signal model can be specified in a straightforward and general (rather than circuit-specific) way. Third, and as a consequence of the foregoing features, the derivation of the model is automatable as demonstrated by the work described in [9].

In our view, these are the features that are critical to distinguishing state-space averaging from the various other approaches to obtaining approximate continuous-time models. They are the features we look for in developing a general approach to modeling the dynamics of a much wider class of circuits. ([4] and [9] also describe how higher order approximations can be obtained, and these refinements can serve to determine approximately such things as the ripple of the waveforms.)

B. Exact Sampled-Data Models and Hybrids

Exact sampled-data (or equivalent) models for the small-signal behavior of switched dc–dc converters have been derived by various workers; see, for example, [10]–[13], [33], and the references therein. Our framework in this paper is closest in spirit to [11] and [13]. We extend their formalism to arbitrary circuits, including those (such as resonant converters) where no fixed natural sampling interval exists (because, for example, the natural sampling interval is itself the control variable).

Various hybrids of the approximate continuous-time and exact sampled-data models have also been described, for example, in [14] and [15]. The objective of these is to find a compromise between the simplicity, directness, and usefulness of the approximate continuous-time models on the one hand and the accuracy of the exact sampled-data models on the other.

The introductory comments in [15] note that the exact sampled-data approach of [13], besides being accurate, is also *general* in scope: it "could be used in any application where the linearization of a periodically changing structure is sought" and "is capable of accurately describing any multistructural nonlinear system by a discrete-time domain model." Our paper can be viewed as a detailed elaboration of the foregoing comments to show (in a broader context than [13]) precisely how the claims in those comments are realized.

C. Other Classes of Circuits

General surveys of analytical techniques for power electronic circuits may be found in [34] and [35]. Sampled-data models for specific circuits in categories other than switched dc–dc converters have, of course, been developed. The dynamics of a controlled rectifier are treated in [16], for example, while the more recent papers [17], [18], and [36] deal with resonant converters which have features that make the construction of exact sampled-data models a little more subtle. (The illustration of our modeling procedure in Section V is based on a series resonant

converter, and the results naturally overlap with those of [17] and to a lesser extent [18], [36]. Our work was carried out independently of the work reported in these papers. However, our interest in dynamic modeling of resonant converters was partially sparked by [19] which dealt with static characteristics.)

III. Power Electronic Circuits as Cyclically Switched Systems

The dynamics of essentially all cyclically operated power electronic circuits can be represented in a straightforward and uniform way if the circuits are modeled as comprising only linear time-invariant (LTI) elements, ideal sources, and ideal switches (whose switching is, however, allowed to be governed by the state of the circuit and by external inputs). This section develops the representation. Several further generalizations, e.g., to the case of nonlinear elements, are also possible, and some of these will be noted later.

We first write down the LTI continuous-time state-space equations that describe the circuit in each of the switch configurations that it goes through in a cycle of operation along with the conditions that determine the transition from one switch configuration to another. This then leads to a sampled-data model that describes the evolution of the state from the beginning of one cycle to the beginning of the next. The durations of the cycles are not constrained to be equal. A particular class of symmetry properties found in many power electronic circuits is also identified, and ways to exploit such symmetry are suggested here and in Section IV.

The section concludes with a discussion of issues related to automatic generation of the models developed here, using both symbolic and numerical procedures. It is pointed out that symbolic procedures may provide attractive possibilities for such automated derivation of models and subsequent analysis.

A. Continuous-Time Description of Circuit Operation

For notational clarity we shall generally use lower case boldface letters to denote vectors and upper case boldface for matrices. The exception will be the use of $\boldsymbol{T}_k$ for the vector of transition times associated with the kth cycle; see the following. Lightface lower and upper case letters will be used to denote scalars.

We consider a power electronic system model that is characterized as follows. The system operates cyclically. In the kth cycle, extending from time $t = t_k$ to time $t = t_{k+1}$, the n-dimensional state vector $\boldsymbol{x}(t)$ of the system is governed by a succession of N LTI state-space equations of the form

$$\frac{d\boldsymbol{x}(t)}{dt} = \boldsymbol{A}_i\boldsymbol{x}(t) + \boldsymbol{B}_i\boldsymbol{u}(t) \qquad t_k + T_{k,i-1} < t \leq t_k + T_{k,i}, \tag{1}$$

one for each of the N switch configurations in the kth cycle. The state $\boldsymbol{x}(t)$ is continuous across each change in switch configuration, i.e., the final state in one configuration is the initial state in the next. (See [32] for a generalization to the case where the number and identity of the state variables is allowed to change from configuration to configuration.) The index i in (1) runs from one to N, with

$$T_{k,0} = 0$$

$$t_{k+1} = t_k + T_{k,N}.$$

Thus $T_{k,N}$ is the duration of the kth cycle.

The $T_{k,i}$ may be termed (relative) *transition times*; they are the times, relative to the start of the kth cycle, at which the switch configurations change. Their dependence on external control action and on the system state will be elucidated shortly. It is advantageous, for both notational and conceptual reasons, to collect the transition times into the N-vector $\boldsymbol{T}_k$:

$$\boldsymbol{T}_k = \begin{bmatrix} T_{k,1} \\ \vdots \\ T_{k,N} \end{bmatrix}.$$

The m-dimensional vector $\boldsymbol{u}(t)$ is a vector of time functions that typically represents sources acting on the circuit, and $\boldsymbol{A}_i$ and $\boldsymbol{B}_i$ in (1) are $n \times n$ and $n \times m$ matrices, respectively.

For a given $\boldsymbol{x}(t_k)$ the evolution of the system (1) in the kth cycle is completely determined by the source waveforms and the transition times at which the switch configurations change. (More will be said in Section III-B about how, in principle, one actually represents and computes this evolution.) In the cases of interest to us these source waveforms and transition times are in turn governed, directly or indirectly, by a set of independent *controlling parameters* $p_{k,j}$. Some of the controlling parameters serve to determine directly all the source waveforms in the vector $\boldsymbol{u}(t)$ for the kth cycle (e.g., these parameters may be the amplitudes and frequencies of fundamentals and harmonics of the sources). The manner in which the controlling parameters determine the transition times $T_{k,i}$ is a little more subtle, as outlined next.

The transition times $T_{k,i}$ are essentially of two types. One type of transition may be *directly controlled* by external control action; this is usually the situation when, for example, thyristors are turned on or transistors are turned on or off (the exceptions correspond to those thyristors or transistors for which these particular operations have been made functions of the system state and are thus no longer direct functions of external control action). The corresponding transition times are then directly and explicitly determined by some of the controlling parameters.

The other type of transition only occurs when the system state reaches particular boundaries or *threshold conditions* (we interpret the term somewhat more narrowly than in [13]); this is the case with, for example, thyristors

turning off (threshold condition: zero thyristor current) or diodes turning on (threshold condition: zero diode voltage) or off (threshold condition: zero diode current). This type of transition is thus only *indirectly or implicitly controlled* by the controlling parameters via the effect of external control action on the state trajectories of the system.

We shall find it advantageous, again for both notational and conceptual reasons, to assemble all the independent controlling parameters into a vector labeled $\boldsymbol{p}_k$. The expressions that give the $\boldsymbol{u}(t)$ in the kth cycle in terms of the entries of $\boldsymbol{p}_k$ are typically simple and explicit. Those that give the $T_{k,i}$ in terms of the entries of $\boldsymbol{p}_k$ can range from simple and explicit to complicated and implicit; simple explicit expressions are to be expected for the directly controlled transitions, while complicated implicit expressions are the norm for the indirectly controlled transitions.

If, for example, the duration $T_{k,N}$ of the kth cycle is itself directly controlled (e.g., because it is determined by our turning on a particular transistor) one might simply have an explicit equation such as

$$T_{k,N} = p_{k,3}$$

to say that the duration of the kth cycle is an entry (the third entry for the specific example cited above) of our vector $\boldsymbol{p}_k$ of independent controlling parameters.

For an example at the other extreme, suppose $T_{k,2}$ is the transition time corresponding to a particular diode turning off and is hence indirectly controlled. The threshold condition in this case occurs when the diode current becomes zero. One can thus first analytically determine an expression for the current in the conducting diode as a function of time (relative to the start of the kth cycle) for the specified $\boldsymbol{x}(t_k)$ and $\boldsymbol{p}_k$. This expression will typically be an exponential/trigonometric function of time. Now $T_{k,2}$ can be specified as the time at which this expression equals zero, which clearly gives rise in the typical case to a complicated and implicit relation between $T_{k,2}$ and the remaining parameters.

Despite the distinction between the two types of transition times the equations relating the N-vector $\boldsymbol{T}_k$ of transition times to the vector $\boldsymbol{p}_k$ of the controlling parameters, for both the directly and indirectly controlled cases and for any given $\boldsymbol{x}(t_k)$, can be seen to be summarized in a set of N equations that has the form

$$\boldsymbol{c}(\boldsymbol{x}(t_k), \boldsymbol{p}_k, \boldsymbol{T}_k) = \boldsymbol{0}. \tag{2}$$

From now on we shall refer to this set as the *constraint equation* for the system. (It is this set that constitutes what are termed the threshold conditions in [13].) More will be said about the form of the constraint equation under "Further Structure" in the following subsection.

Note that the compact and innocuous notation $\boldsymbol{c}(\cdot\ ,\ \cdot\ ,\ \cdot)$ is being used to denote a vector function of three vector arguments: the N-vector $\boldsymbol{c}(\cdot\ ,\ \cdot\ ,\ \cdot)$ is actually

$$\boldsymbol{c}(\cdot\ ,\ \cdot\ ,\ \cdot) = \begin{bmatrix} c_1(\cdot\ ,\ \cdot\ ,\ \cdot) \\ \vdots \\ c_N(\cdot\ ,\ \cdot\ ,\ \cdot) \end{bmatrix},$$

where each of the $c_i(\cdot\ ,\ \cdot\ ,\ \cdot)$ is a scalar function of three vector arguments. The power of the notation lies in the fact that the resulting formulas, both already mentioned and in what follows, look exceedingly simple, and the development of the analysis is kept transparent. The detailed fussing over the circuit-specific forms and entries of the vector functions can be left to a later (and preferably automated) stage of the derivation.

Sensitivity to System Parameters: A generalization of viewpoint will actually enable us, with no increase in notational burden, to represent the effect of system parameters such as inductor, capacitor, and resistor values on system behavior. Simply consider those parameters for which such sensitivity information is desired to be additional components of $\boldsymbol{p}_k$, the vector of independent controlling parameters. The expressions developed in the rest of the paper will then contain the relationships needed to determine sensitivity of behavior to system parameters.

B. Large-Signal Sampled-Data Description

On integrating the governing description (1) over the interval from t_k to t_{k+1} and noting that $\boldsymbol{u}(t)$ in the kth cycle is directly determined by $\boldsymbol{p}_k$, a *sampled-data description* of the form

$$\boldsymbol{x}(t_{k+1}) = \boldsymbol{f}(\boldsymbol{x}(t_k), \boldsymbol{p}_k, \boldsymbol{T}_k) \tag{3}$$

is obtained. (This is the case even if the number or identity of the state variables is allowed to change from configuration to configuration in the kth cycle.) Again, note that the symbol $\boldsymbol{f}(\cdot\ ,\ \cdot\ ,\ \cdot)$ is being used to denote an n-vector, each of whose entries is a scalar function of three vector arguments. The integration referred to earlier can, in the case of (1), be represented analytically in more detail as discussed under "Further Structure" to follow.

For given $\boldsymbol{x}(t_k)$ and specified controlling parameters $\boldsymbol{p}_k$ the constraint (2) may be used to determine $\boldsymbol{T}_k$, typically by an iterative numerical computation (since some of the component equations of (2) will typically be implicit nonlinear equations). Substitution of the resulting $\boldsymbol{T}_k$ in (3) then yields the state $\boldsymbol{x}(t_{k+1})$ at the beginning of the next cycle. The process is then continued forward. We thus have in (2), (3) an exact large-signal sampled-data description of the dynamics of any power electronic circuit that can be modeled via (1). The circuit treated in Section V, see (24) and (25), provides a concrete example of a model of the form (2), (3); see also [36] for a more leisurely and detailed development of the large-signal sampled-data model for essentially the same circuit.

If only the small-signal model that describes perturbations about a nominal cyclic steady state is of interest (see Section IV), then this sort of computation is used only to find numerically the steady state itself. Various issues arise in solving implicit nonlinear systems of the form (2),

but discussion of these is deferred to Section IV where some of the issues are brought up in connection with numerical computation of the steady state.

Further Structure: A sampled-data relation of the form (3) and the associated constraint (2) actually exist for systems that are far more general than those specified by (1). For example, relations of the form (2), (3) would in principle exist if each LTI equation of the type (1) was replaced by a *nonlinear* time-invariant equation. This could certainly occur in power electronic circuits of interest due, for example, to significant nonlinearity in inductors or because of essential nonlinearities in the models used for electromechanical or other loads connected to the power electronics (see the cases treated in [37] and [38]).

However, the special case specified via (1) is what is most commonly considered in the power electronics literature, and in this case the sampled-data model has further structure which can and should be exploited. Equation (3) now takes the form

$$\boldsymbol{x}(t_{k+1}) = \boldsymbol{F}(\boldsymbol{p}_k, \boldsymbol{T}_k)\boldsymbol{x}(t_k) + \boldsymbol{g}(\boldsymbol{p}_k, \boldsymbol{T}_k) \tag{4}$$

where the $n \times n$ matrix $\boldsymbol{F}(\cdot\ ,\ \cdot)$ and the n-vector $\boldsymbol{g}(\cdot\ ,\ \cdot)$ are *analytically representable* in terms of and computable from the $\boldsymbol{A}_i$, $\boldsymbol{B}_i$, and $\boldsymbol{u}(t)$ of (1), using matrix exponentials involving the $\boldsymbol{A}_i$ and associated integrals. This can be proven and the precise formulas determined by piecing together the usual "variation of parameters" formula for the solution of (1); see, for example, [20, p. 368] and the particular cases treated in [13].

Furthermore, if the variables (such as thyristor currents or diode currents and voltages) that determine the threshold conditions for the indirectly controlled transition times are linear in the state variables, then (2) also takes the related form

$$\boldsymbol{C}(\boldsymbol{p}_k, \boldsymbol{T}_k)\boldsymbol{x}(t_k) + \boldsymbol{d}(\boldsymbol{p}_k, \boldsymbol{T}_k) = \boldsymbol{0} \tag{5}$$

where, again, the $N \times n$ matrix $\boldsymbol{C}(\cdot\ ,\ \cdot)$ and the N-vector $\boldsymbol{d}(\cdot\ ,\ \cdot)$ are representable in terms of and computable from the $\boldsymbol{A}_i$, $\boldsymbol{B}_i$, and $\boldsymbol{u}(t)$ of (1), along with knowledge of the matrices that specify how the state variables and source vectors are related to the variables that determine the threshold conditions. Again, the computations involve matrix exponentials in the $\boldsymbol{A}_i$ and associated integrals. As with (2) some of the N equations that constitute (5) will be simple and explicit expressions relating some of the $T_{k,i}$ to entries of $\boldsymbol{p}_k$, while others will be more complicated implicit constraints.

Analytically explicit representations of the type (4), (5) do not normally exist for models more general than (1), and one is then forced to fall back on *numerically determined* versions of the model (2), (3). In this situation one has to integrate numerically whatever differential equations take the place of (1), monitoring the values of variables that determine the threshold conditions, and switching differential equations as appropriate when these thresholds are crossed.

Auxiliary Variables: It is often the case that one also wants to model the evolution of certain variables other than the state variables. For example, one may wish to examine how the average value of some variable, taken over a cycle, varies as one goes from cycle to cycle (see [17] for an analysis of such a case), or one may be interested in the dynamic evolution of the peak value in each cycle of some variable. Any auxiliary variable in which the value for the kth cycle is determined entirely by system behavior in the kth cycle is completely determined by $\boldsymbol{x}(t_k)$, $\boldsymbol{p}_k$, and $\boldsymbol{T}_k$. Collecting all such auxiliary variables of interest into a vector $\boldsymbol{y}_k$, one can obtain an equation of the form

$$\boldsymbol{y}_k = \boldsymbol{h}(\boldsymbol{x}(t_k), \boldsymbol{p}_k, \boldsymbol{T}_k) \tag{6}$$

to be considered along with (2) and (3). The constraint (2) can be used, as before, to eliminate $\boldsymbol{T}_k$ from (6) as needed. Note again that the notation $\boldsymbol{h}(\cdot\ ,\ \cdot\ ,\ \cdot)$ represents a vector function of three vector arguments.

The special form of the model (1) induces further structure on the foregoing expression for the auxiliary variables of interest if these variables are linear functions of the state variables. In this case (6) takes the form

$$\boldsymbol{y}_k = \boldsymbol{H}(\boldsymbol{p}_k, \boldsymbol{T}_k)\boldsymbol{x}(t_k) + \boldsymbol{m}(\boldsymbol{p}_k, \boldsymbol{T}_k) \tag{7}$$

see (4) and (5). The matrix $\boldsymbol{H}(\cdot\ ,\ \cdot)$ and the vector $\boldsymbol{m}(\cdot\ ,\ \cdot)$ are computable from the $\boldsymbol{A}_i$, $\boldsymbol{B}_i$, and $\boldsymbol{u}(t)$ of (1), along with knowledge of the matrices that specify how the auxiliary variables are related to the state vector and source variables.

C. Exploiting Symmetry

Many power electronic circuits possess various symmetry properties that may be exploited to provide more economical and powerful model descriptions and to reduce computational effort. Stimulated by some arguments in [17], we discuss one class of symmetries here (and continue the discussion of it in Section IV), but undoubtedly other classes exist that are worth exploring.

It is not uncommon for a complete cycle of circuit operation to be composed of a basic pattern that is repeated a certain number of times with some special transformation of the pattern at each repetition within the cycle. For concreteness and simplicity of exposition we restrict ourselves here to the frequently encountered case of two pattern repetitions per cycle, which we shall label *half-cycle symmetry*. Our treatment has a natural extension to the case of more than two patterns per cycle, and the details can be fairly directly worked out once the case of half-cycle symmetry is properly understood.

Assume that the first half-cycle of the kth cycle is described by equations of the form

$$\boldsymbol{x}(t_{2k+1}) = \boldsymbol{f}_h(\boldsymbol{x}(t_{2k}), \boldsymbol{p}_{2k}, \boldsymbol{T}_{2k}) \tag{8a}$$

and

$$\boldsymbol{c}_h(\boldsymbol{x}(t_{2k}), \boldsymbol{p}_{2k}, \boldsymbol{T}_{2k}) = \boldsymbol{0}. \tag{8b}$$

(The dummy index k runs through all integer values as before.) These are obtained by exactly the same line of argument used to obtain (2) and (3), with a sequence of

LTI equations as in (1) now used to describe evolution of the system state in the first half-cycle of the kth cycle, and so on. Thus the only difference from (2) and (3) is a change of time variable that lets us count by half-cycles instead of cycles so that we can consider samples at the end of every half-cycle rather than at the end of every cycle.

A number of power electronic circuits with two patterns per cycle, i.e., with half-cycle symmetry, have the property that the evolution in the second half-cycle is governed by the same functions $f_h(\cdot\ ,\ \cdot\ ,\ \cdot)$ and $c_h(\cdot\ ,\ \cdot\ ,\ \cdot)$ acting on a *transformed state* vector in the following special way:

$$\boldsymbol{Wx}(t_{2k+2}) = f_h(\boldsymbol{Wx}(t_{2k+1}),\ p_{2k+1},\ T_{2k+1}) \tag{9a}$$

and

$$c_h(\boldsymbol{Wx}(t_{2k+1}),\ p_{2k+1},\ T_{2k+1}) = \mathbf{0} \tag{9b}$$

with

$$\boldsymbol{W}^2 = \boldsymbol{I} \text{ the identity matrix so } \boldsymbol{W}^{-1} = \boldsymbol{W}. \tag{9c}$$

The matrix $\boldsymbol{W}$ (which acts as a "square root" of the identity matrix) could, for example, be a diagonal matrix with 1's and -1's on its diagonal, or a block diagonal matrix with blocks of the form

$$\begin{bmatrix} 0 & +1 \\ +1 & 0 \end{bmatrix}$$

or

$$\begin{bmatrix} 0 & -1 \\ -1 & 0 \end{bmatrix}$$

on its diagonal along with 1's and -1's. The part played by the condition (9c) on $\boldsymbol{W}$ only becomes evident when considering the cyclic steady state; see Section IV. (Further generalizations involving not only more patterns per cycle but also transformations of the controlling parameters p_k as well, can certainly be considered but are omitted here.)

Thus for a circuit of this class one only need obtain the large-signal dynamic model over a half-cycle rather than over the whole cycle, i.e., obtain the $f_h(\cdot\ ,\ \cdot\ ,\ \cdot)$ and $c_h(\cdot\ ,\ \cdot\ ,\ \cdot)$ of (8) and (9). The scheme that specifies how the pattern should be repeated to make the cycle, i.e., the scheme embodied in $\boldsymbol{W}$, then yields the model over the full cycle. This enables sampled-data representation of dynamics over a finer grid (namely, on a pattern-by-pattern rather than a cycle-by-cycle basis) and can also reduce the work involved in obtaining and using a dynamic model of the circuit. Further exploitation of this kind of symmetry in constructing the small-signal model is demonstrated in Sections IV and V.

The role of appropriate notation in specifying the aforementioned type of symmetry in a general way and in analyzing its consequences is worth noting. The power of appropriate notational tools, unfortunately, often tends to be underestimated.

D. Automatability

The key steps in the foregoing procedure can certainly be automated. The approach in [9] for automated derivation of state-space-averaged models of switched converters from circuit descriptions indicates the sort of route that may be followed in the more general setting considered here (and in Section IV).

We shall in our discussions consider both numerical computations and *symbolic* ones (i.e., those that preserve chosen parameters in symbolic form without substituting in their numerical values till called on to do so). The use of computers in power electronic design is normally associated with numerical computations. However, the growing availability of symbolic manipulation languages such as Macsyma [21] and SMP [22] on smaller and smaller computers and the evolving capabilities of these languages make it attractive to consider their use in automated model derivation and analysis procedures for problems such as ours. (Macsyma—Project MAC's symbolic manipulation system—is a computer programming system written in Lisp and used for performing symbolic as well as numerical mathematical manipulations. It originated at MIT but is now very widely disseminated and used.) It should *not* be construed that the results in this paper *require* symbolic manipulation programs. The intent here is only to point out that the sorts of operations called for in our treatment are particularly suited to the capabilities of symbolic manipulation programs.

The potential advantages of a symbolic analysis over a numerical one include the possibility of developing greater insight into the problem and solution, as well as the fact that solving the problem for a new choice of parameter values now usually involves only substitution and evaluation, rather than starting the analysis again from scratch. Note that even advanced symbolic analysis programs often fail to recognize ways to collapse or simplify the elaborate expressions that they frequently produce, thereby undermining the first of the potential advantages mentioned earlier.

Essentially all the computations involved in deriving the model for the series resonant converter example in Section V, starting with a state-space description of the system in the form (1) and going via the sampled-data descriptions (4), (5), and (7) to the small-signal model given by the expressions in (15) of Section IV, were carried out using Macsyma, yielding a symbolically specified model. Thus each time a different set of circuit-parameter values is given the new description (4), (5), and (7) is evaluated by simple numerical substitution for the symbols, and the new small-signal model is determined as soon as the cyclic steady state (see (10) of Section IV) has been computed numerically for the specified parameters. The time and cost involved in generating the symbolic model on Macsyma were minimal.

Table I shows a sample interaction with Macsyma. The matrix exponential of a 2×2 matrix $\boldsymbol{A}$ (the one that actually arises in our example in Section V) is computed symbolically, i.e., in terms of symbols denoting the ele-

TABLE I
SAMPLE INTERACTION WITH MACSYMA

```
(c1) A:MATRIX([0,1/C],[-1/L,0]);

        [  0    1/C ]
(d1)    [           ]
        [ -1/L   0  ]

(c2) S:MATRIX([s,0],[0,s]);

        [ s  0 ]
(d2)    [      ]
        [ 0  s ]

(c3) SA:S-A;

        [  s   -1/C ]
(d3)    [           ]
        [ 1/L    s  ]

(c4) ISA:SA^-1;

        [    CLs          L      ]
        [ ---------   ---------  ]
        [    2           2       ]
        [ CLs  + 1    CLs  + 1   ]
(d4)    [                        ]
        [     C          CLs     ]
        [ - --------  ---------  ]
        [    2           2       ]
        [ CLs  + 1    CLs  + 1   ]

(c5) A11:ISA[1,1];

            CLs
(d5)     ---------
            2
         CLs  + 1

(c6) ILT(A11,s,t);
Is CL positive, negative or zero?

pos;

(d6)          cos(sqrt(CL)t/CL)

(c7) INTEGRATE (d6(t),t);
Is CL positive, negative or zero?

pos;

(d7)         CLsin(sqrt(CL)t/CL)
             -------------------
                  sqrt(CL)

    ... etc.
```

Lines labeled (c1), etc., are those typed in by user; those labeled (d1), etc., are Macsyma responses. The labels can also be used to refer to the lines—see the use of d6 in (c7).

This is Macsyma 303, © Copyright 1976, 1983 Massachusetts Institute of Technology.

ments of the original matrix, by taking the inverse Laplace transform (ILT in statement (c6) of Table I) of $(sI-A)^{-1}$ Symbolic integrals (INTEGRATE in statement (c7) of Table I) and derivatives of the matrix exponential are also easily obtained. The user can choose which, if any, of the problem parameters are to be treated symbolically; for instance, the matrix A in our example can be specified entirely numerically and the matrix exponential $\mathbf{exp}\ (At)$ computed in terms of the symbol t.

Scores of other Macsyma features can be used for symbolic analysis. In addition, assorted numerical computations and plotting routines can be carried out within Macsyma itself. Macsyma is not restricted to running interactively and can be run in batch mode as well. It should be evident from the illustration here that the availability of such a language opens up possibilities for a style of automated analysis that is radically different and potentially much richer than one based on numerical computations alone.

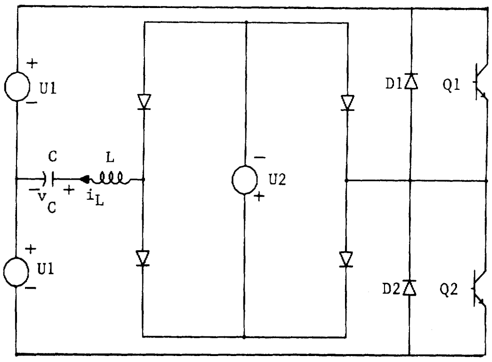

Fig. 1. Simple series resonant converter; L = 197 μH, C = 100 nF, $U1$ = 14 V, f_r = 35.8 kHz, f_s = 40 kHz (unless otherwise specified).

Work already exists in the literature of computer-aided circuit analysis and design on the topic of symbolic analysis. Examples can be seen in [20] and [23] where some approaches in this vein are developed; their focus, however, is on symbolic generation of network functions of linear systems. New factors will undoubtedly enter in the context of power electronics but remain to be systematically explored and exploited. One point to be kept in mind is that the circuit models in power electronics for which usable dynamic models are desired typically contain far fewer elements than the circuits encountered in signal-processing applications. Hence analysis approaches that may be deemed impractical for the latter (perhaps because of the possibility of exponential growth in computational effort with a number of symbols) may well be eminently useful for the former.

We return now to examine the specific computations of interest to us here. The procedure for going from a power electronic circuit description and a given switching sequence to the state-space equations (1) is well established [20], [23], [9]. It is quite feasible to obtain these equations automatically, not only numerically, but also in symbolic form.

The major task in obtaining (4), (5), and (7) from (1) is that of computing matrix exponentials and integrals involving them. The example in Table I has already indicated that this can be done symbolically. Much has been written on the topic of *numerically* computing matrix exponentials. Many proposed algorithms behave poorly numerically (see the title of [24]), but sound algorithms exist that have been developed by numerical analysts [24], [25].

Symbolic solution of (4) to obtain $\boldsymbol{T}_k$ in terms of $\boldsymbol{x}(t_k)$ and $\boldsymbol{p}_k$ may not always be possible, given the complicated implicit form of some of the threshold conditions. However, numerical algorithms for solution of nonlinear equations are well established; see [20] and [23].

As already mentioned in Section III (under "Further Structure"), if the LTI descriptions in (1) are replaced by *nonlinear* time-invariant descriptions, the potential for symbolic computations is drastically reduced because no computable "nonlinear version" of the matrix exponential exists; the solution over an interval now has to be specified numerically, in general.

IV. Perturbations About a Nominal Cyclic Steady State

Most power electronic circuits are designed to operate nominally in some *cyclic steady state* with a suitable corresponding choice of controlling parameters and a regular sequence of switch transitions. The dynamics of *perturbations* about this steady state determine the stability of the steady state and the response to disturbances. If the dynamics are unstable, this steady state cannot be maintained without corrective control action. This is the reason for using "nominal" to describe the cyclic steady state; it is a steady state that may not be attained without control action to stabilize perturbations. A small-signal model to describe perturbations about the nominal cyclic steady state is crucial to properly designing a feedback controller. This section first discusses the determination of steady-state conditions for the models of Section III and then shows how the required small-signal model can be constructed.

A. The Cyclic Steady State

If a power electronic system model of the form (1) has a nominal cyclic steady state, then

$$\boldsymbol{x} = \boldsymbol{f}(\boldsymbol{x}, \boldsymbol{p}, \boldsymbol{T}) \tag{10a}$$

and

$$\boldsymbol{c}(\boldsymbol{x}, \boldsymbol{p}, \boldsymbol{T}) = \boldsymbol{0} \tag{10b}$$

for the functions $\boldsymbol{f}(\cdot\ ,\ \cdot\ ,\ \cdot)$ and $\boldsymbol{c}(\cdot\ ,\ \cdot\ ,\ \cdot)$ defined in (2), (3) with vectors $\boldsymbol{x}$, $\boldsymbol{p}$, and $\boldsymbol{T}$ that denote *constant* steady-state values of the sampled state, controlling parameters, and transition times:

$$\boldsymbol{p}_k = \boldsymbol{p} \tag{11a}$$

$$\boldsymbol{T}_k = \boldsymbol{T} \tag{11b}$$

(with corresponding constant cycle *duration* $T_{k,N} = T_N$) and

$$\boldsymbol{x}(t_k) = \boldsymbol{x}(kT_N) = \boldsymbol{x}. \tag{11c}$$

The conditions in (10) follow from the fact that a cyclic steady state is characterized by values of the controlling parameters and initial state such that the system, after excursions and changes of switch configuration, returns at the end of the cycle to the same state.

While the vectors $\boldsymbol{x}$, $\boldsymbol{p}$, and $\boldsymbol{T}$ that characterize a cyclic steady state of the power electronic circuit model will always satisfy (10), the converse is not true: many solutions $\boldsymbol{x}$ and $\boldsymbol{T}$ of the implicit nonlinear system in (10) may exist for a given $\boldsymbol{p}$, but it is *not* necessary that all of them (or even *any* of them if the circuit in fact has no nominal cyclic steady state) correspond to possible nominal cyclic steady states of the circuit. Some solutions of the system of equations may not be physically meaningful; if, for example, any entry of $\boldsymbol{T}$ is negative, or if the ith entry is smaller than the $(i\text{-}1)$th for some i, the solution is physically meaningless, as can be seen from the definition of the $T_{k,i}$ in (1). Furthermore, even solutions that one cannot immediately rule out on physical grounds need not correspond to nominal cyclic steady states.

It therefore becomes necessary to use additional information and knowledge of the circuit to decide which solutions of (10) for a given $\boldsymbol{p}$ correspond to valid nominal cyclic steady states. This may come from rough estimates of $\boldsymbol{x}$ and $\boldsymbol{T}$ for the specified $\boldsymbol{p}$, provided by time-domain simulation or approximate analysis. Such estimates are in fact also very important in providing candidate solutions of (10) in the first place because the usual iterative algorithms (such as the popular Newton–Raphson procedure [13], [20], [23], and [37]) for determining solutions of the nonlinear equations in (10) require adequate estimates to get started.

If the nominal steady state is stable, one can obtain estimates of steady-state characteristics by simulating the system from some initial condition until it reaches the steady state. This can be computationally expensive if done digitally, particularly when the circuit's convergence to the steady state is relatively slow. Alternative simulation approaches such as use of MIT's Parity Simulator [26] provide a useful alternative to digital simulation for this purpose. If the nominal steady state happens to be unstable, other methods must be used. Some recent computational approaches to determining the nominal cyclic steady state are discussed in [23].

B. Dynamics of Perturbations from Steady State

Assume that a particular nominal cyclic steady state has been computed and that a model to represent the dynamics of perturbations from this steady state is desired. We shall use the following notation to represent perturbations of the various system variables from their steady state values in (11):

$$\begin{aligned} \boldsymbol{x}_k &= \boldsymbol{x}(t_k) - \boldsymbol{x} \\ \boldsymbol{q}_k &= \boldsymbol{p}_k - \boldsymbol{p} \\ \boldsymbol{r}_k &= \boldsymbol{T}_k - \boldsymbol{T} \\ \tau_k &= T_{k,N} - T_N. \end{aligned} \tag{12}$$

Note that τ_k is the perturbation in the duration of the kth cycle and is actually the last component of $\boldsymbol{r}_k$.

From (2) and (3) we then get

$$\boldsymbol{x}_{k+1} = \boldsymbol{f}(\boldsymbol{x} + \boldsymbol{x}_k, \boldsymbol{p} + \boldsymbol{q}_k, \boldsymbol{T} + \boldsymbol{r}_k) - \boldsymbol{x} \tag{13a}$$

with

$$\boldsymbol{c}(\boldsymbol{x} + \boldsymbol{x}_k, \boldsymbol{p} + \boldsymbol{q}_k, \boldsymbol{T} + \boldsymbol{r}_k) = \boldsymbol{0}. \tag{13b}$$

Carrying out (multivariable) Taylor series expansions in (13), retaining only linear terms, and using (10) yields what is essentially the desired small-signal model (though still in implicit form):

$$\boldsymbol{x}_{k+1} = [\partial \boldsymbol{f}/\partial \boldsymbol{x}]\boldsymbol{x}_k + [\partial \boldsymbol{f}/\partial \boldsymbol{p}]\boldsymbol{q}_k + [\partial \boldsymbol{f}/\partial \boldsymbol{T}]\boldsymbol{r}_k \tag{14a}$$

and

$$[\partial \boldsymbol{c}/\partial \boldsymbol{x}]\boldsymbol{x}_k + [\partial \boldsymbol{c}/\partial \boldsymbol{p}]\boldsymbol{q}_k + [\partial \boldsymbol{c}/\partial \boldsymbol{T}]\boldsymbol{r}_k = \boldsymbol{0}. \tag{14b}$$

Once again, the compact notation makes things look simple, but power over the symbols requires understanding them completely. The (derivative or Jacobian) symbol $[\partial f/\partial x]$ is being used to denote an $n \times n$ *matrix* in which the ith row, jth column entry is the partial derivative of the ith entry of the vector $f(\cdot\ ,\ \cdot\ ,\ \cdot)$ with respect to the jth entry of its first vector argument evaluated at the cyclic steady state specified by x, p, and T. If we consider the special form of (3) that is given in (4), then $[\partial f/\partial x] = F(p, T)$. Similar definitions hold for the other matrices of derivatives in (14). Note that $[\partial c/\partial T]$ is a square matrix.

The equations in (14) can be combined by solving for r_k from (14b) and substituting the resulting expression in (14a) to get

$$x_{k+1} = F_o x_k + G_o q_k \tag{15a}$$

where

$$F_o = [\partial f/\partial x] - [\partial f/\partial T]\,[\partial c/\partial T]^{-1}[\partial c/\partial x] \tag{15b}$$

and

$$G_o = [\partial f/\partial p] - [\partial f/\partial T]\,[\partial c/\partial T]^{-1}[\partial c/\partial p]. \tag{15c}$$

This constitutes the final form of the LTI sampled-data model for perturbations of the system away from a cyclic steady state. In particular, the cyclic steady state is locally asymptotically stable (without further control action) if and only if all eigenvalues of F_o have magnitude less than one. Recall also from Section III that expressions for sensitivity to system parameter perturbations are included in (15) if these system parameters have in turn been included in the vector of controlling parameters p_k.

Note that alternative ways to combine the equations in (14) may exist, resulting in state-space descriptions involving some other choice of n variables from the set of $n + N$ variables x_k and r_k. A sampled-data model of this form, with perturbations in a certain conduction time as one of the state variables, is developed in [18] for a particular resonant converter.

Auxiliary Variables: Perturbations of the auxiliary variables in (6) from their steady-state values $y = h(x, p, T)$ can also be readily modeled. Defining (cf. (11), (12))

$$v_k = y_k - y, \qquad y = h(x, p, T), \tag{16}$$

we get (by the same procedure of Taylor expansion in (6), truncation at linear terms, and use of (16) and (14b)):

$$v_k = H_o x_k + J_o q_k \tag{17a}$$

where

$$H_o = [\partial h/\partial x] - [\partial h/\partial T][\partial c/\partial T]^{-1}[\partial c/\partial x] \tag{17b}$$

and

$$J_o = [\partial h/\partial p] - [\partial h/\partial T][\partial c/\partial T]^{-1}[\partial c/\partial p]. \tag{17c}$$

Frequency Domain Expressions: One can now examine such things as the transfer function matrix that relates the z transform of the *sequence* v_k to that of the *sequence* q_k:

$$R(z) = H_o(zI - F_o)^{-1}G_o + J_o.$$

These sequences are samples of underlying continuous-time physical waveforms. While our formulation permits small cycle-time perturbations τ_k away from the nominal steady-state period T_N (see (11) and (12) for definitions of these variables), the perturbations x_k in $x(t_k)$ given by (15) can actually be considered as occurring *at* the nominal sampling instants, provided the τ_k are small enough compared to T_N. This then enables standard sampled-data frequency-domain methods [27], [28] to be used to relate the frequency-domain behavior of (15) and of the auxiliary equations (17) to that of the underlying system. The key step in such frequency-domain studies is to consider the response of (15) and (17) to controlling parameter perturbations of the form

$$q_k = e^{jk\theta}q_0$$

for θ in the range $[0, \pi]$. This leads (for study of the sequence v_k) to examination of $R(e^{jk\theta})$.

Exploiting Symmetry: Circuits with two patterns per cycle that possess the symmetry property defined in the previous section via (8) and (9) are typically designed to have a steady state x, p, T such that if the system starts in the state x at the beginning of a cycle, it is in the state Wx at the end of the first half-cycle and finishes up back at x at the end of the cycle. It follows, from the specified behavior over the first half-cycle and using (8), that

$$Wx = f_h(x, p, T) \tag{18a}$$

and

$$c_h(x, p, T) = 0. \tag{18b}$$

Recall that $f_h(\cdot, \cdot, \cdot)$ and $c_h(\cdot, \cdot, \cdot)$ represent behavior over a half-cycle rather than over a cycle. Then using (9), including the condition (9c) that $W^2 = I$ (so that $W^{-1} = W$), shows that the state at the end of the second half-cycle, i.e., at the end of the cycle, is indeed x again so that no further equations need to be written to complete the specification of the cyclic steady state.

Perturbing the model (8), (9) about the steady state then yields small-signal models for x_k over the odd and even half-cycles. These perturbation models over the two half-cycles are *not the same* (though they happen to be related by what is termed a "similarity transformation" involving W). However, considering the sequence obtained by taking x_{2k} at even half-cycle times and Wx_{2k+1} at odd half-cycle times yields the following *uniform model* that serves our purposes completely:

$$s_{i+1} = WF_o s_i + WG_o q_i \tag{19a}$$

where

$$s_{2k} = x_{2k} \text{ and } s_{2k+1} = Wx_{2k+1} \tag{19b}$$

and F_o and G_o are given by expressions of the form (15b) and (15c) except that $f_h(\cdot, \cdot, \cdot)$ and $c_h(\cdot, \cdot, \cdot)$ are used instead of $f(\cdot, \cdot, \cdot)$ and $c(\cdot, \cdot, \cdot)$. If one can observe and control the system on a pattern-by-pattern basis, the

model (19) is what is needed to permit exploitation of the doubled system bandwidth. The foregoing treatment clarifies and generalizes the somewhat *ad hoc* explanation of notational choice in [17].

Automatability: Numerical algorithms for determining both the cyclic steady state and the partial derivatives that are required to compute the small-signal model are well established [13], [20], [23], [37]. It should also be apparent from the discussion in Section III that Macsyma can perform all the operations (partial differentiation, matrix inversion, multiplication, etc.) needed to construct the small-signal model of (15)–(18) in *symbolic* form (starting from the structures in (4), (5), and (7)) with the steady-state values $\boldsymbol{x}$, $\boldsymbol{p}$, and $\boldsymbol{T}$ retained as symbols (along with other variables for which one may wish to defer substitution of numerical values). The numerical small-signal model can then be evaluated by simple substitution once the cyclic steady-state has been numerically computed.

V. Application to a Series Resonant Converter

The development in the preceding sections is illustrated here by application to the simple series resonant converter circuit shown in Fig. 1. Our original interest in dynamic modeling was stimulated by resonant converters, but the results here are *not* aimed at a detailed elucidation of the properties of these circuits. For such detailed studies of resonant converter dynamics refer to [17]–[19], [29], [30], [36], [40], and the references therein.

Basic Features: The transistor/diode pairs $Q1/D1$ and $Q2/D2$ function as switches that cause the voltage $U1$ from the split dc source to be applied with alternating polarities across the series combination of inductor L, capacitor C, and the diode bridge. The dc voltage source $U2$ in the diode bridges constitutes the load and aids or opposes $U1$, depending on the polarity of the inductor current i_L. The magnitude of the steady-state response of the series LC pair, and hence the average current through the load, is clearly related to how much the switching frequency f_s differs from the resonant frequency $f_r = 1/2\,\pi\sqrt{LC}$. The switching frequency (or, equivalently, the switching period) is the primary control variable for such circuits.

Observed Dynamics: Before proceeding with an analysis of the circuit it is useful to demonstrate that it does indeed have interesting behavior that calls for explanation. The (oscilloscope and plotter) waveforms here and later have been obtained on MIT's Parity Simulator [26].

The lower trace in Fig. 2(a) and (b) shows the load current (which is just the rectified inductor current) when the switching frequency is varied in accordance with the upper trace. The figure gives the responses to step changes in switching frequency for different operating conditions. The higher frequency in each case is above resonance, but in Fig. 2(b) the frequency drops below resonance as well. The envelopes display typical response characteristics of underdamped second-order systems. Furthermore, the envelope in Fig. 2(b) shows behavior that would be ascribed

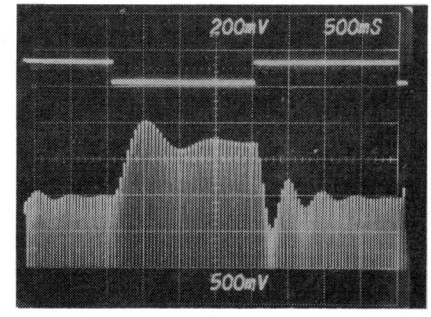

(a)

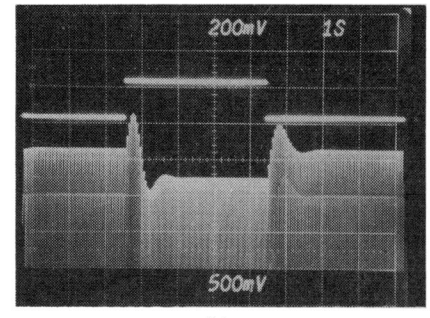

(b)

Fig. 2. Response of rectified inductor current to step changes in switching frequency. (a) Load voltage $U2 = 0.2$ V and switching frequency f_s steps between 44 kHz and 39.6 kHz. (b) Load voltage $U2 = 5$ V and switching frequency f_s steps between 40 kHz and 32 kHz.

to a real right-half-plane zero in a continuous-time system, namely an initial kick in the direction opposite the value to which it eventually settles. Simulations have shown that the large-signal behavior of the circuit can get considerably more complicated, but we omit these waveforms.

Circuit Operation: Evidently, the inductor current and capacitor voltage are the natural state variables for this circuit. Their waveforms over a cycle of operation are shown in Fig. 3 for the case where $f_s > f_r$; for our purposes here it is adequate to restrict ourselves to this case of *switching above resonance*. In this case the diodes and transistors conduct in the sequence $D1$, $Q1$, $D2$, $Q2$. The precise evolution of the system is described next. We only consider in detail the circuit's behavior over a half-cycle, since the circuit operates with half-cycle symmetry (as will be confirmed shortly).

As soon as $Q2$ is turned off (and $Q1$ turned on), marking the end of the $(2k-1)$th half-cycle or $(k-1)$th cycle, $D1$ begins to conduct, marking the beginning of the $2k$th half-cycle. $D1$ eventually turns off at the (relative) transition time $T_{2k,1}$, when its current $i_L(t)$ reaches the threshold value of zero, and $Q1$ begins to conduct. Thus $T_{2k,1}$ corresponds to an *indirectly controlled* transition, implicitly determined by the threshold condition

$$i_L(T_{2k,1}) = 0. \tag{20a}$$

At time $T_{2k,2}$, $Q1$ is turned off (and $Q2$ turned on), thereby starting the $(2k+1)$th half-cycle and causing $D2$ to begin conducting. Hence $T_{2k,2}$, corresponds to a

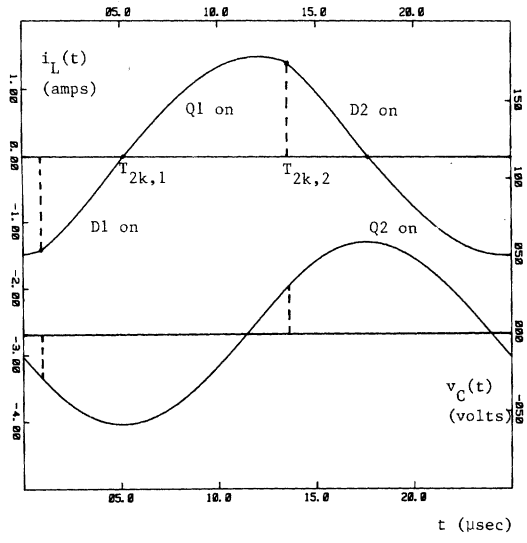

Fig. 3. State variable waveforms ($U2$ = 2 V).

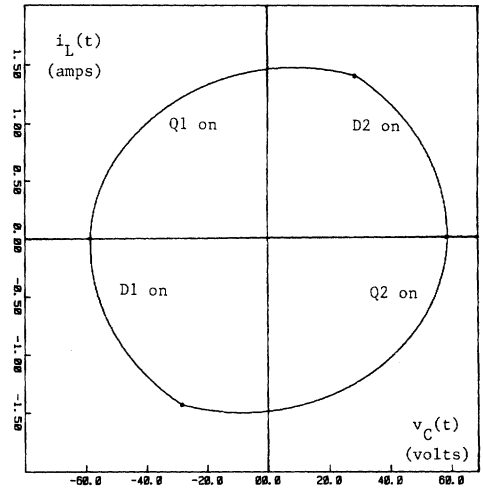

Fig. 4. Phase plane plot ($U2$ = 2 V).

directly controlled transition, and we shall, for later convenience, consider it to be related to the first controlling parameter for this half-cycle in the following way:

$$T_{2k,2} - 1/(2p_{2k,1}) = 0. \tag{20b}$$

(We shall eventually be setting $p_{2k,1}$ to be the switching frequency in the kth cycle.)

If interest exists in the *sensitivity* of the circuit to time-varying perturbations in $U1$ and $U2$ as well as to deviations in L and C from their nominal values, it is merely necessary to label these variables as controlling parameters before applying the formulas developed in Sections III and IV:

$$\begin{aligned} p_{2k,2} &= U1_{2k} \\ p_{2k,3} &= U2_{2k} \\ p_{2k,4} &= L \\ p_{2k,5} &= C. \end{aligned} \tag{20c}$$

It is evident that the equations in (20) constitute the constraint equation set for this circuit; see (8b).

Continuous-Time Description: The sequence of state equations of the form (1) that governs the circuit over the first half-cycle of every cycle is particularly simple. Taking the state vector to be

$$\boldsymbol{x}(t) = \begin{bmatrix} v_C(t) \\ i_L(t) \end{bmatrix}, \tag{21}$$

we find that in each of the two switch configurations of the half-cycle the system has the same $\boldsymbol{A}_i$ matrix, namely

$$\boldsymbol{A}_1 = \boldsymbol{A}_2 = \begin{bmatrix} 0 & 1/C \\ -1/L & 0 \end{bmatrix} \tag{22}$$

while the input vector (corresponding to the term $\boldsymbol{B}_i\boldsymbol{u}(t)$ in (1)) is given by

$$\begin{bmatrix} 0 \\ (U1 + U2)/L \end{bmatrix} \tag{23a}$$

when $D1$ is conducting, and

$$\begin{bmatrix} 0 \\ (U1 - U2)/L \end{bmatrix} \tag{23b}$$

when $Q1$ is conducting.

In the second half-cycle of each cycle the transformed vector $-\boldsymbol{x}(t)$ satisfies the same set of equations that $\boldsymbol{x}(t)$ did in the first half-cycle, so that the circuit displays precisely the half-cycle symmetry treated earlier with the matrix $\boldsymbol{W}$ of (9c) being simply $-\boldsymbol{I}$ where $\boldsymbol{I}$ is now the 2×2 identity matrix.

Sampled-Data Description: From the foregoing continuous-time description it is possible to write down quite directly the sampled-data description in (8a) by using the matrix exponential of the $\boldsymbol{A}$ of (22) and integrals of this matrix exponential acting on the inputs in (23). Our analysis actually did this using Macsyma and verified the results by direct computation. However, because of the simple nature of the circuit in Fig. 1, a more transparent route to the solution is obtained by using the following easily proven characterization of the phase-plane diagram of this particular circuit.

If $(\sqrt{L/C})i_L$ is plotted against v_C on the same scale, then the system trajectories (even under *transient* conditions) consist of a sequence of *circular arcs*, each arc centered on the v_C axis at a voltage equal to that applied across the LC pair during the segment of the trajectory under consideration.

A phase-plane diagram of inductor current i_L versus capacitor voltage v_C in the steady state, again obtained from the Parity Simulator, is shown in Fig. 4. Whatever the route chosen for analysis, the result obtained is the following (written with all inessential subscripts dropped

for notational simplicity):

$$x(T_2) = \begin{bmatrix} \cos(wT_2) & Z_0 \sin(wT_2) \\ -[\sin(wT_2)/Z_0] & \cos(wT_2) \end{bmatrix} x(0) + \begin{bmatrix} V1[\cos(wT_2 - wT_1) - \cos(wT_2)] + V2[1 - \cos(wT_2 - wT_1)] \\ V1[\sin(wT_2) - \sin(wT_2 - wT_1)]/Z_0 + V2[\sin(wT_2 - wT_1)]/Z_0 \end{bmatrix} \tag{24}$$

where $V1 = U1 + U2$, $V2 = U1 - U2$, $w = 1/\sqrt{LC}$, and $Z_0 = \sqrt{L/C}$. The condition (20a) can also be expanded into

$$i_L(T_1) = [-(1/Z_0)\sin(wT_1) \quad \cos(wT_1)]x(0) + [V1 \sin(wT_1)]/Z_0 = 0. \tag{25}$$

Equations (24) and (25) make explicit what the functions $f_h(\cdot, \cdot, \cdot)$ and $c_h(\cdot, \cdot, \cdot)$ of (9) are for this example.

Steady State: The general iterative approach to computing numerically the cyclic steady state for this circuit via (18) can be followed using (20) and (24). Computation of static characteristics of such a converter is also discussed in [19]. It turns out, however, that the simple phase-plane trajectories of the particular circuit being considered here actually permit a direct *closed-form* solution of the steady state. The details are not hard to work out and are presented in [30].

Small-Signal Sampled-Data Model: Putting the foregoing all together, and performing the necessary linearization, one arrives at a model of the form (19) to describe the evolution of the system in terms of samples taken every half-cycle. If, however, all the controlling parameters are constrained to vary no more frequently than once per cycle, which is typical for operation of this circuit, it will be convenient to work in terms of a model that samples once per cycle. This model is directly obtained by merely applying (19) twice in succession. Using the fact that $\boldsymbol{W} = -\boldsymbol{I}$ in our case, writing $\boldsymbol{x}_k$ now to denote the perturbation at the onset of the kth *cycle* and $\boldsymbol{q}_k$ the perturbation in the controlling parameters in the kth cycle, and with $\boldsymbol{F}_o$ and $\boldsymbol{G}_o$ as defined in (19), we get

$$\boldsymbol{x}_{k+1} = \boldsymbol{F}_o^2 \boldsymbol{x}_k + [\boldsymbol{F}_o - \boldsymbol{I}]\boldsymbol{G}_o \boldsymbol{q}_k. \tag{26}$$

This is the model we use in describing the following results.

Results: The small-signal model (26) can now be used to study in detail the dynamics of perturbations about the cyclic steady state for various operating conditions. Some examples of the sorts of results one might wish to compute are given next.

Fig. 5(a) shows the locus of natural frequencies or poles $z_{p,1}$ and $z_{p,2}$ (which are just the eigenvalues of $\boldsymbol{F}_o^2$) for the discrete-time system (26) as the load voltage $U2$ varies. Mapping these back to "equivalent" continuous-time poles $f_s \ln(z_{p,i})$ in the usual way [13], [27], [28] we get Fig. 5(b). An interesting feature of the loci is that for small $U2$ the poles are lightly damped and at the *difference* between the switching and resonant frequencies. It is essentially at this difference frequency that the envelope of the resonant current is observed to ring in response to a small step change in forcing frequency. (A direct explanation of this can be found in the limiting linear case of $U2 = 0$.) Elaboration on our observation here may be found in [29] and [41].

Fig. 6 shows the gain and phase of the transfer function from perturbations $q_{k,1}$ in the switching frequency to perturbations in the sampled inductor current $x_{k,2}$. The locus (not shown here) of the zero of this transfer function, as the load $U2$ is varied, indicates that the zero starts on the negative real axis inside the unit circle, becomes increasingly negative as $U2$ is increased, and actually wraps around at infinity to return along the positive real axis. For $U2 = 5$ V, which is the condition shown in Fig. 2(b), the zero is at around 18; since this is on the real axis to the right of the unit circle, an initial excursion in the opposite direction to the final value is to be expected and is observed in Fig. 2(b).

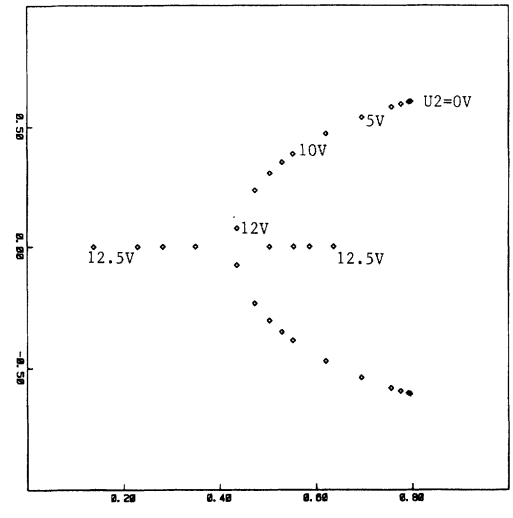

(a)

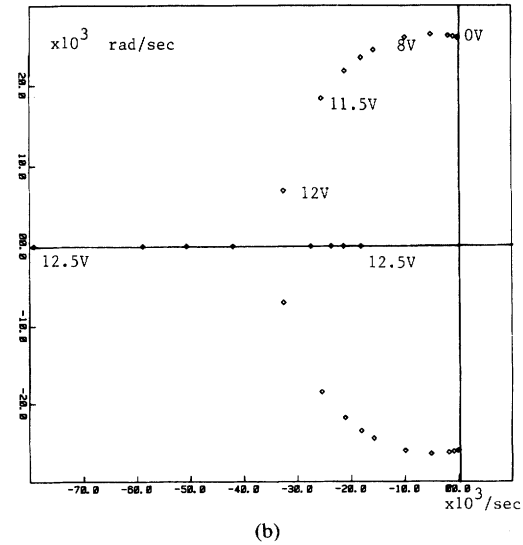

(b)

Fig. 5. (a) Locus of discrete-time system poles as load voltage $U2$ varies. (b) "Equivalent" continuous-time poles.

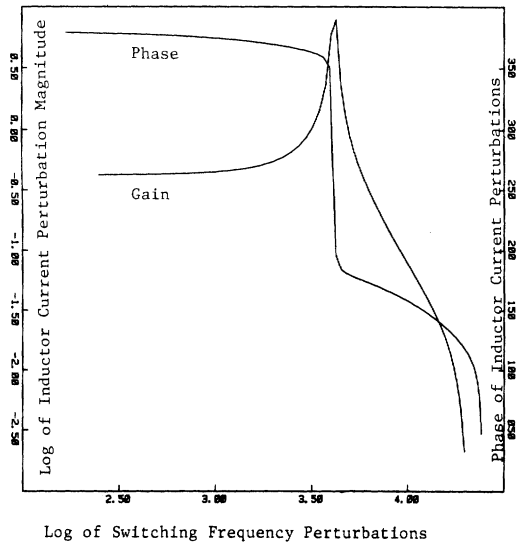

Fig. 6. Bode plot of small-signal model ($U2$ = 0.2 V).

Acknowledgment

The authors are grateful to several MIT/Industry Power Electronics Collegium members for continuing encouragement, and to Dr. J. Wilson of General Electric in particular.

References

[1] G. W. Wester and R. D. Middlebrook, "Low-frequency characterization of switched dc-dc converters," *IEEE Trans. Aerosp. Electron. Syst.*, vol. AES-9, pp. 376-385, May 1973.

[2] R. D. Middlebrook and S. Cuk, "A general unified approach to modeling switching converter power stages," in *IEEE Power Electronics Specialists' Conf. Rec.*, 1976, pp. 18-34.

[3] M. Clique and A. J. Fossard, "A general model for switching converters," *IEEE Trans. Aerosp. Electron. Syst.*, vol. AES-13, pp. 397-400, July 1977.

[4] M. Grotzbach, "Analysis of periodically switch controlled lowpass systems by continuous approximation models," *Automatica*, vol. 17, pp. 321-334, 1981.

[5] G. Verghese and U. Mukherji, "Extended averaging and control procedures," in *IEEE Power Electronics Specialists' Conf. Rec.*, 1981, pp. 329-336.

[6] U. Itkis, *Control Systems of Variable Structure*. New York: Wiley, 1976.

[7] F. Harashima, H. Hashimoto, and S. Kondo, "MOSFET converter-fed position servo system with sliding mode control," in *IEEE Power Electronics Specialists' Conf. Rec.*, 1983, pp. 73-79.

[8] G. Guardabassi, A. Locatelli, and S. Rinaldi, "Status of periodic optimization of dynamic systems," *J. Optimiz. Theory Appl.*, vol. 14, 1974.

[9] R. J. Dirkman, "Generalized state-space averaging," in *IEEE Power Electronics Specialists' Conf. Rec.*, 1983, pp. 283-294.

[10] A. Capel, J. G. Ferrante, and R. Prajoux, "Dynamic behaviour and z-transform stability analysis of dc/dc regulators with a nonlinear PWM control loop," in *IEEE Power Electronics Specialists' Conf. Rec.*, 1973, pp. 149-157.

[11] ——, "State-variable stability analysis of multi-loop PWM controlled dc/dc regulators in light and heavy mode," in *IEEE Power Electronics Specialists' Conf. Rec.*, 1975, pp. 91-103.

[12] H. Buhler, "Study of a dc chopper as a sampled system," in *Proc. 2nd IFAC Symp. Control in Power Electronics and Electrical Drives*, 1977, pp. 67-77.

[13] F. C. Y. Lee, R. P. Iwens, Y. Yu, and J. E. Triner, "Generalized computer-aided discrete-time modeling and analysis of dc-dc converters," *IEEE Trans. Industr. Electron. Contr. Instrum.*, vol. IECI-26, pp. 58-69, May 1979.

[14] A. R. Brown and R. D. Middlebrook, "Sampled-data modeling of switching regulators," in *IEEE Power Electronics Specialists' Conf. Rec.*, 1981, pp. 349-369.

[15] D. J. Shortt and F. C. Lee, "Extensions of the discrete-average models for converter power stages," in *IEEE Power Electronics Specialists' Conf. Rec.*, 1983, pp. 23-37.

[16] J. P. Sucena-Paiva, R. Hernandez and L. L. Freris, "Stability study of controlled rectifier using a new discrete model," *Proc. Inst. Elec. Eng.*, vol. 119, pp. 1285-1293, 1972.

[17] V. Vorperian and S. Cuk, "Small signal analysis of resonant converters," in *IEEE Power Electronics Specialists' Conf. Rec.*, 1983, pp. 269-282.

[18] S. W. H. de Haan, "A new integral pulse module for the series-resonant converter," *IEEE Trans. Ind. Electron.*, vol. IE-31, pp. 255-262, Aug. 1984.

[19] V. Vorperian and S. Cuk, "A complete dc analysis of the series resonant converter," in *IEEE Power Electronics Specialists' Conf. Rec.*, 1982, pp. 85-100.

[20] L. O. Chua and P.-M. Lin, *Computer-Aided Analysis of Electronic Circuits*. Englewood Cliffs, NJ: Prentice-Hall, 1975.

[21] *MACSYMA Reference Manual*, Mathlab Group, Laboratory for Computer Science, Massachusetts Inst. Technol. Cambridge, 1983.

[22] SMP (Symbolic Manipulation Program), Inference Corporation, Los Angeles, CA.

[23] J. Vlach and K. Singhal, *Computer Methods for Circuit Analysis and Design*. New York: Van Nostrand Reinhold, 1983.

[24] C. B. Moler and C. Van Loan, "Nineteen dubious ways to compute the exponential of a matrix," *SIAM Rev.*, vol. 20, 1978.

[25] C. Van Loan, "Computing integrals involving the matrix exponential," *IEEE Trans. Automat. Contr.*, vol. AC-23, pp. 395-404, June 1978.

[26] J. G. Kassakian, "Simulating power electronic systems—A new approach," *Proc. IEEE*, vol. 67, pp. 1428-1439, Oct. 1979.

[27] G. F. Franklin and J. D. Powell, *Digital Control of Dynamic Systems*. Reading MA: Addision Wesley, 1980.

[28] K. J. Astrom and B. Wittenmark, *Computer Controlled Systems: Design and Analysis*. Englewood Cliffs, NJ: Prentice-Hall, 1984.

[29] V. Vorperian, "Analysis of resonant converters," Ph.D. dissertation, Power Electronics Group, California Inst. of Technol., Pasadena, May 1984.

[30] M. E. Elbuluk, "Resonant converters: Topologies, dynamic modeling and control," Ph.D. dissertation Dep. Elec. Eng. Comput. Sci. Massachusetts Inst. Technol., Cambridge, May 1986.

[31] J. P. Louis, "Nonlinear and linearized models for control systems including static converters," in *Proc. 3rd. IFAC Symp. Control in Power Electronics and Electrical Drives*, Sept. 1983, pp. 9-16.

[32] R. von Lutz and M. Grotzbach, "Straightforward discrete modelling for power converter systems," in *IEEE Power Electronics Specialists' Conf. Rec.*, 1985, pp. 761-770.

[33] P. Maranesi and V. Varoli, "Exact continuous models of PWM regulators in both continuous and discontinuous conduction modes," in *Rec. European Space Agency Sessions*, held in conjunction with IEEE Power Electronics Specialists' Conf., 1985, pp. 235-238.

[34] S. B. Dewan and G. R. Slemon, "Analysis techniques for thyristor converters," in *IEEE Power Electronics Specialists' Conf. Rec.*, 1973, pp. 141-148.

[35] R. G. Hoft and J. B. Casteel, "Power electronic circuit analysis techniques," presented at 2nd IFAC Symp. Control in Power Electronics and Electrical Drives, Dusseldorf, 1977; reprints available from Prof. Hoft, Univ. Missouri-Columbia, Columbia, MO.

[36] R. J. King and T. A. Stuart, "Large-signal dynamic simulation for the series resonant converter," *IEEE Trans. Aerosp. Electron. Syst.*, vol. AES-19, pp. 859-870, Nov. 1983.

[37] H. Haneda, Y. Kuroe, and T. Maruhashi, "Computer-aided analysis of power-electronic dc-motor drives: Transient and steady-state analysis," in *IEEE Power Electronics Specialists' Conf. Rec.*, 1982, pp. 128-139.

[38] K. Shinohara and S. Nonaka, "Stability improvement of a current source inverter-induction motor drive system," in *Proc. 3rd IFAC Symp. Control in Power Electronics and Electrical Drives*, Sept. 1983, pp. 329-336.

[39] R. W. Brockett and J. R. Wood, "Electrical networks containing controlled switches," *Supplement to IEEE Symp. Circuit Theory*, Apr. 1974.

[40] R. Oruganti and F. C. Lee, "State plane analysis of parallel resonant converter," *IEEE Power Electronics Specialists' Conf. Rec.*, 1985, pp. 56-73.

[41] V. Vorperian, "High-Q approximations in the small-signal analysis of resonant converters," *Power Electronics Specialists' Conf. Rec.*, 1985, pp. 707–715.

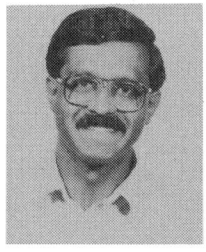

George C. Verghese (S'74–M'78) was born in Ethiopia. He received the B.Tech degree from the Indian Institute of Technology, Madras, India in 1974, the M.S. degree from the State University of New York, Stony Brook, in 1975, and the Ph.D. degree from Stanford University, Stanford, CA, in 1979, all in electrical engineering.

He is an Associate Professor of Electrical Engineering and a member of the Laboratory for Electromagnetic and Electronic Systems at the Massachusetts Institute of Technology, Cambridge. His research interests are in the areas of systems, control, and estimation, especially as applied to power electronics, electrical machines, and bulk power systems.

Dr. Verghese is an Associate Editor of *Automatica*, the journal of the International Federation of Automatic Control.

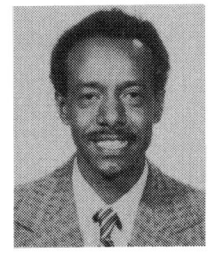

Malik E. Elbuluk (S'79) was born in Wadmedani, Sudan, in 1953. He received the B.Sc. degree in electrical engineering from the University of Khartoum, Sudan, in 1976, and the M.S. and E.E. degrees in electrical engineering from the Massachusetts Institute of Technology (MIT), Cambridge, in 1980 and 1981, respectively. He is currently completing the Ph.D. degree at MIT on the topic of resonant converter topologies, dynamic modeling, and control.

His research interests are in power electronics.

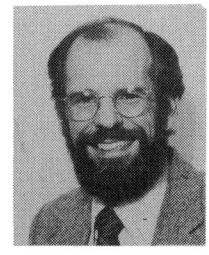

John G. Kassakian (S'65–M'73–SM'80) received the B.S., M.S., and Sc.D. degrees from the Massachusetts Institute of Technology (MIT), Cambridge, in 1965, 1968, and 1973, respectively.

From 1969 to 1971 he was on active duty in the U.S. Navy. He is currently a Professor of Electrical Engineering at MIT. In addition, he is the Director of the MIT/Industry Power Electronics Collegium and Associate Director of the Laboratory for Electromagnetic and Electronic Systems at MIT. His research is in the area of power electronics with current work aimed at system simulation, effects and elimination of converter-generated harmonics, characterization of new semiconductor devices, application of microprocessors to the control of static converter systems, high-frequency energy conversion, and high-performance machine drives.

Dr. Kassakian is a member of Tau Beta Pi, Eta Kappa Nu, and Sigma Xi.